ARTICLES

Effect of pressure on the crystal structure, vibrational modes, and electronic excitations of HgO

T. Zhou and U. Schwarz
Max-Planck-Institut für Festkörperforschung, Heisenbergstrasse 1, D-70569 Stuttgart, Germany

M. Hanfland
European Synchrotron Radiation Facility, BP 220, F-38043 Grenoble Cedex, France

Z. X. Liu, K. Syassen, and M. Cardona
Max-Planck-Institut für Festkörperforschung, Heisenbergstrasse 1, D-70569 Stuttgart, Germany

(Received 28 July 1997)

We have investigated the effect of pressure on structural properties, lattice vibrations, and electronic excitations of HgO using x-ray-diffraction and optical spectroscopies. At 14(1) GPa orthorhombic HgO undergoes a first-order phase transition. The diffraction diagram of the high-pressure phase can be indexed assuming a tetragonal cell. Its structure is a distorted variant of the NaCl-type structure. Pronounced softening of oxygen-related Raman modes is observed in both the low- and high-pressure phases. Photoluminescence spectra indicate that the band gap of orthorhombic HgO decreases with increasing pressure, in accordance with the redshift of band-edge-related features seen in optical reflectivity. Above 28 GPa, the optical reflectivity of the high-pressure phase shows an increase of the near-infrared oscillator strength, indicating the onset of a metallic regime. [S0163-1829(98)01802-5]

I. INTRODUCTION

Recent systematic high-pressure studies of II-VI semiconductors using angle-dispersive diffraction techniques have revealed several new structures and phase transitions,[1] leading to new insights in the structural systematics of these materials as well as prompting computational studies of the structural behavior using *first principle* methods.[2] Among the II-VI semiconductors, mercury oxide probably is the most unusual one in terms of its ambient-pressure structural properties. These are largely determined by the strong tendency for linear coordination of Hg when forming Hg-O bonds.

We report a high-pressure investigation of the structural properties, vibrational modes, and electronic excitations of HgO. The primary motivation was to study the structural stability of HgO and to develop an overall picture of the pressure-induced changes of its electronic structure. Pressure-induced phase transitions of mercury(II)-chalcogenides (sulfide, selenide, and telluride) have been studied in some detail.[3] The common transition sequence in these compounds for increasing pressure was given as zinc blende (phase I), cinnabar (phase II), NaCl-type (phase III), and body-centered tetragonal (phase IV).[3] In phase III these materials were found to become metallic.[4] More recently, McMahon *et al.* have discovered a distorted zinc-blende-type structure between phase I and phase II in HgSe and HgTe.[5]

HgO crystallizes in the orthorhombic space group $Pnma(D_{2h}^{16})$.[6,7] The structure is built up of planar -O-Hg-O- zigzag chains running parallel to the a axis and lying in the ac plane (see Fig. 1). Within a chain the Hg atoms are linearly coordinated by two oxygen atoms at a distance $d \sim 203$ pm. One unit cell contains two chains lying on two adjacent ac planes, resulting in four formula units per cell.[6] The closest interchain Hg-O distances are 287 pm within ac planes and 282 pm for neighboring ac planes. HgO shows a reddish color.[8] The band gap energy is approximately 2.2 eV at room temperature,[10] and n-type electrical conductivity has been reported.[11,12]

As for the high-pressure behavior of HgO, Shchennikov and co-workers[11,12] measured the magnetoresistance, electrical resistance, and thermoelectric power of HgO in synthetic diamond chambers at pressures up to 35 GPa. They reported

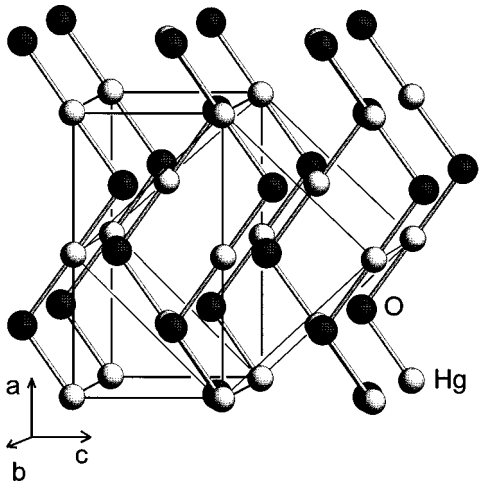

FIG. 1. View of the crystal structure of orthorhombic HgO. Axes directions and the orthorhombic unit cell are indicated as well as a larger cell which illustrates the relation to the NaCl-type structure. The lattice parameters at ambient pressure are $a=661$ pm, $b=552$ pm, and $c = 352$ pm.

 © 1998 The American Physical Society

a semiconductor-metal transition at pressures close to 10 GPa. Voronin and Shchennikov[13] performed an x-ray-diffraction investigation of HgO samples retrieved after a pressure cycle. The x-ray-diffraction patterns indicated a change from the orthorhombic to a tetragonal structure when the maximum applied pressure was larger than 10 GPa. More recently, the high-pressure properties of HgO were investigated by means of extended x-ray-absorption fine structure (EXAFS) and energy-dispersive x-ray diffraction.[14] Three phase transitions were reported at 2 GPa, 5 GPa, and 13 GPa, respectively.

We have performed angle-dispersive x-ray-diffraction experiments with a sealed x-ray source as well as synchrotron radiation. No indications were found of phase transformations in HgO which had been reported to occur at 2 GPa or 5 GPa. Our x-ray results indicate a discontinuous structural change at $P \sim 14(1)$GPa. The diffraction data of the high-pressure phase are interpreted in terms of a tetragonal structure. Our Raman study shows consistent behavior, in that the only region of discontinuous frequency changes takes place near 14 GPa. Pronounced phonon softening of oxygen-related modes is observed throughout the pressure range up to 34 GPa. In order to obtain information on the electronic properties of HgO at high pressures, we measured photoluminescence (PL) and optical reflectivity spectra of HgO up to 6 and 34 GPa, respectively. The main finding is that pressure reduces the band gap and that HgO undergoes an electronic transition to a metallic state near 28 GPa. This paper is organized as follows: After giving some experimental details, we present the x-ray-diffraction results, then discuss the pressure dependence of Raman modes, and finally address the optical properties and band gap changes of HgO. A preliminary account of the present work was given elsewhere.[15]

II. EXPERIMENTAL DETAILS

The polycrystalline samples were single-phase orthorhombic HgO, as confirmed by standard powder x-ray diffraction. Diamond anvil cells (DAC's) with beryllium and metal backing plates were used for diffraction and optical spectroscopies, respectively. Pressure was measured *in situ* using the ruby luminescence method.[16] In x-ray-diffraction and Raman experiments a 4:1 ethanol/methanol mixture served as pressure medium. Low-temperature PL measurements of single-crystal samples (grown by a vapor transport method) were measured using helium as the pressure medium. For optical reflectivity experiments, a 20-μm–thick layer of HgO powder was loaded into the DAC's and then covered with CsCl powder.

Angle-dispersive x-ray-diffraction diagrams were obtained with a sealed source (Ag $K\alpha$ radiation, graphite monochromator) or synchrotron radiation (BL3 at the ESRF, 50 pm wavelength) using image plate detector systems. The two-dimensional diffraction patterns were converted to intensity versus 2Θ data by means of the programs Platypus[17] or Fit2d.[18] Indexing, lattice parameter determination, and full profile refinements were performed using the program system CSD.[19]

Raman spectra were excited at 514.5 nm and recorded employing a triple spectrograph and a multichannel detector.

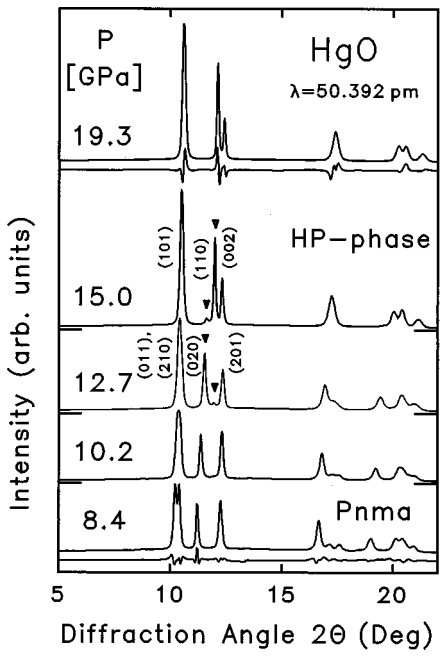

FIG. 2. Powder x-ray-diffraction diagrams of polycrystalline HgO at different pressures between 8.4 and 19.3 GPa. The triangles point to a reflection of the high-pressure phase appearing at 12.7 GPa and to a reflection of the low-pressure phase which has almost disappeared at 15.0 GPa. Below the patterns at 8.4 GPa and 19.3 GPa we also show the deviation of the refined profiles from the experimental data.

Photoluminescence spectra (514.5 nm excitation) were measured up to 6 GPa at 10 K using a germanium detector operating at 77 K or a photomultiplier detector. Optical reflectivity spectra were taken in the range 0.6–4 eV using a micro-optical system described elsewhere.[20]

III. CRYSTAL STRUCTURE

Angle-dispersive x-ray-diffraction experiments of HgO were carried out at various pressures up to 19.3 GPa. Initial diffraction experiments with a laboratory setup indicated the evolution of a higher-pseudosymmetry at pressures above 8 GPa. For this reason, higher-resolution measurements were performed using synchrotron radiation at the ESRF, aiming to resolve small peak splittings and detect possible superstructure reflections.

The lower diagram in Fig. 2 shows a diffraction pattern of HgO measured at 8.4 GPa. With these experimental data we performed a full-profile refinement using the space group and atomic positions of orthorhombic HgO at ambient pressure and taking into account preferred orientation effects. The difference between measured and refined intensities (see Fig. 2) corresponds to a very acceptable intensity R value of $R_I = 0.045$. Thus, the low-pressure modification of HgO is stable at pressures well above 5.0 GPa, a result which has been confirmed recently.[21]

Further compression of HgO causes differences in line shifts such that some orthorhombic reflection pairs [e.g., the (011) and (210) reflections] are not clearly resolved at pressures above 10 GPa. Near $P \approx 12.7$ GPa new reflections start to appear. A further increase of pressure induces

intensity changes of both the original and the new reflections, which are consistent with a two-phase region extending from about 12.5 GPa to 15 GPa. The similarity of diffraction diagrams of the high-pressure phase stable above 15 GPa to that of the low-pressure phase indicates a close structural relationship between the two modifications, the diagram of the high-pressure phase showing a smaller number of lines in comparison to the low-pressure form.

Diffraction patterns of the high-pressure phase can be indexed assuming a tetragonal cell with $\sqrt{2}a_t \approx c_t$ [at 15.0(5) GPa, $a_t = 340.2(1)$ pm, $c_t = 468.3(1)$ pm]. We note that this is not the tetragonal phase which was found during the investigation of pressure-recovered samples.[13] Systematic extinctions observed in the diagrams are compatible with a body-centered lattice and calculations using reasonable densities result in $Z = 2$ formula units per unit cell.

We performed a refinement of experimental intensities measured at 19.3 GPa in the space group $I4/mmm$. Full-profile refinements with $a = 337.0(1)$ pm, $c = 465.1(2)$ pm, mercury at position (0,0,0), and oxygen at position (0,0,0.5) converged quickly, yielding residuals for intensities and profiles of $R_I = .057$ and $R_{pr} = 0.174$ (19.3 GPa). Due to the special c/a ratio of the unit cell, the crystal structure deviates only slightly from a tetragonally distorted rocksalt-type arrangement of HgO.

The plot of the differences between observed and calculated intensities at 19.3 GPa (see Fig. 2) shows systematic deviations of line positions and intensities, as are also indicated by the high value of R_{pr}. Also, Bragg peaks of the high-pressure phase with indices $(h0l)$ are systematically broader than other reflection groups; e.g., the (101) reflection has a full width at half maximum (FWHM) of 0.17° compared to a FWHM of 0.1° for the (110) and (002) reflections. Such deviations may be caused not only by the effects of twinning and deviatoric stress, but also by a small distortion of the crystal structure from tetragonal symmetry. In fact, a deviation from the $I4/mmm$ symmetry with $Z = 2$ is indicated by first-order Raman activity of the high-pressure modification of HgO (see Sec. IV).

Since superstructures normally show in peak broadening *and* in extra reflections, special care was taken to look for weak lines, especially at low 2Θ angles. However, examination of diagrams measured in the stability range of the high-pressure modification at pressures up to 20 GPa did not show any extra peaks; i.e., attempts to find an unambiguous evidence for a larger unit cell failed. Thus, we performed test refinements in noncentrosymmetric space groups of tetragonal and orthorhombic symmetry using the cell parameters of the $I4/mmm$ structure as starting values. These attempts did not result in improved fits. We note here that especially a deviation of the oxygen partial structure from the assigned positions or a disorder in oxygen positions cannot be excluded due to the large difference in x-ray-scattering factors of Hg and O. Nevertheless, we consider the proposed tetragonal structure to give a proper description for the *average* structure.

Figure 3 shows lattice parameters and volume per formula unit as a function of pressure. The lattice parameter changes clearly demonstrate a highly anisotropic compressibility of the low-pressure phase. Solid lines in the top frame of Fig. 3 correspond to least squares fits to a linear relation with a slope of $-0.1(1)$ pm/GPa for the a_0 axis and to a quadratic polynomial for the b_0 and c_0 axes with linear coefficients of -4.3 pm/GPa and -2.9 pm/GPa, respectively. The different compressions of the orthorhombic unit cell axes can be explained qualitatively by considering the different bond types within and between the Hg-O chains: The strong compressibility of the b_0 axis is a result of the soft interchain interactions which are found along the [010] direction. The stiffness of the a_0 axis is caused by the [100] orientation of the covalently bonded zigzag chains. The compressibility of the c_0 axis is intermediate due to the fact that we find both soft interchain and covalent intrachain interactions in this direction.

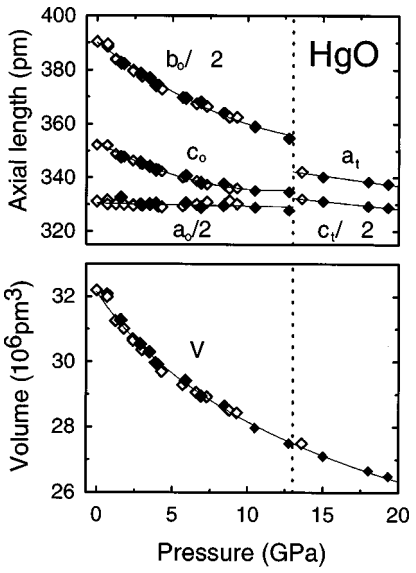

FIG. 3. Pressure dependence of lattice parameters and volume per formula unit of HgO as determined by x-ray-diffraction measurements. Laboratory and synchrotron data are represented by open and solid symbols, respectively. The solid lines are results of least squares fits (see text). The dashed line indicates the phase transition pressure.

The pressure coefficients of the tetragonal axes a_t and c_t of the high-pressure phase are both equal to $-0.08(2)$ pm/GPa. In space group $I4/mmm$ the smallest possible Hg-O distance is $c_t/2 \approx 233$ pm as compared to 203 pm in the orthorhombic structure at $P = 0$ GPa. Thus, the metrical changes at the phase transition indicate the breakdown of the twofold coordination of Hg. However, the fact that the tetragonal c/a ratio is slightly smaller than $\sqrt{2}$ indicates that some degree of anisotropic bonding persists in the high-pressure phase.

The lattice parameters show discontinuous changes at the phase transition, but the volume change is smaller than the experimental uncertainty of about 0.5%. The pressure-volume data up to 19.3 GPa can be fitted by a single Murnaghan-type relation. The solid line in Fig. 3(b) corresponds to parameter values of $V_0 = 32.15 \times 10^6$pm^3, $B_0 = 44(1)$ GPa, and $B' = 7(1)$, where V_0, B_0, and B' are the volume per formula unit, the bulk modulus, and its pressure derivative, respectively, at zero pressure.

Our results regarding the phase stability of HgO disagree with those obtained in recent investigations by means of EXAFS and energy-dispersive powder x-ray diffraction.[14] In or-

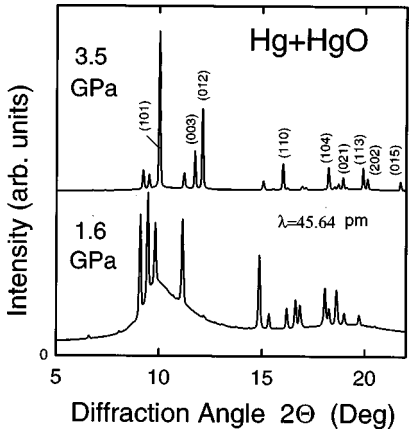

FIG. 4. Synchrotron x-ray-diffraction diagrams obtained for an HgO sample at 1.6 and 3.5 GPa. Diffraction peaks in the lower diagram originate from orthorhombic HgO, while the broad peak in the background is attributed to liquid mercury. The indexed reflections in the upper diagram correspond to solid mercury (rhombohedral structure, indexing in hexagonal setting).

der to clarify the situation, we briefly discuss synchrotron diffraction data obtained at pressures below 6 GPa (see Fig. 4). At $P<2$ GPa, in addition to reflections from orthorhombic HgO, a pronounced background feature is observed with a broad maximum at $2\Theta\approx 10°$. Above 2 GPa strong new lines appear, and the corresponding d values agree with the results of Ref. 14. However, several features of the diagrams are inconsistent with an attribution to a structural transformation of HgO: (1) The d values of all lines which are present below 2 GPa exhibit smooth changes up to 14 GPa with no apparent discontinuity at 2 GPa, (2) the relative intensities of reflections present below 2 GPa remain almost constant up to about 13 GPa, (3) experiments performed with a sealed x-ray source do not show the appearance of extra lines, and (4) synchrotron data measured with initial sample pressures of $P>8$ GPa or with nitrogen as pressure-transmitting medium exhibit only reflections of the orthorhombic low-pressure phase of HgO (up to 12.5 GPa).

The broad background feature in the lower diagram of Fig. 4 is attributed to the presence of liquid mercury, and the pressure at which the new lines appear indeed corresponds to the crystallization pressure of mercury. At 3.5 GPa, the extra lines can be indexed (see Fig. 4) on the basis of a small hexagonal cell ($a=334.2$ pm, $c=682.8$ pm), and intensity calculations show good agreement between the diffraction diagram of α-Hg and the additional features in experimental diagrams. Thus we conclude that the changes at 2.0 GPa do not indicate a phase transition of HgO, but the crystallization of mercury metal. Similarly, changes in diffraction diagrams which were reported to take place near 5 GPa (Ref. 14) can be attributed to a structural transformation from the α to the β modification of mercury.[22] It is not clear yet whether the mechanism leading to the partial decomposition of HgO under monochromatic x-ray irradiation involves excited electronic states or local heating of the lattice.[23] It should be stressed here that a considerable amount of disproportionation of HgO is observed although only monochromatic radiation was used. Similar effects are more likely to occur in energy-dispersive diffraction experiments, where a more intense ''white'' beam impinges on the sample.

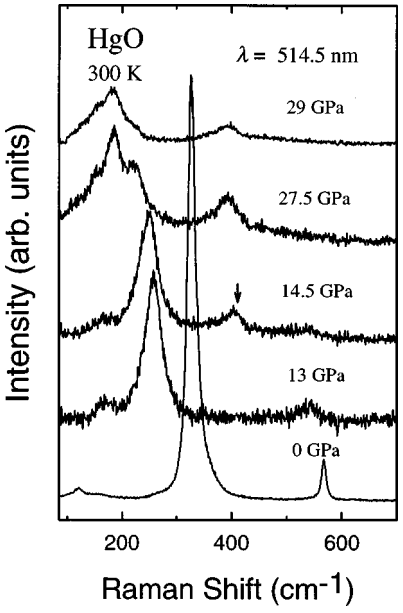

FIG. 5. Raman spectra of polycrystalline HgO at different pressures ($T=300$ K) obtained in nonpolarized configuration. The incident light is the 514.5 nm line of an Ar^+ ion laser. The arrow points at the new mode appearing at the structural phase transition.

IV. RAMAN MODES

Raman spectra of polycrystalline HgO were measured at different pressures up to 34 GPa, and selected spectra are displayed in Fig. 5. In the range 0–10 GPa, the overall scattering intensity decreases continuously, probably due to electronic band gap changes (see Sec. V) and a related decrease of the light penetration depth at the laser wavelength of 514 nm. The Raman mode frequencies were determined from

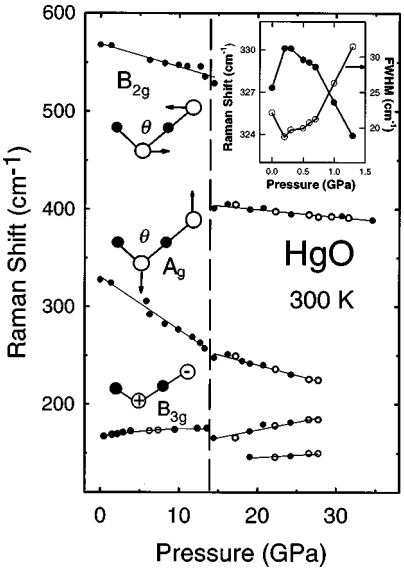

FIG. 6. Pressure dependence of the Raman mode frequencies of polycrystalline HgO determined from fitting Lorentzian line shapes to the measured spectra. The dashed line at 14 GPa marks the pressure of the structural phase transition. Solid and open circles represent data from upward and downward runs, respectively. The inset shows the Raman shift (solid symbols) and linewidth (open circles) of the A_g mode at low pressures.

fitting Lorentzians to the measured spectra, and the pressure dependence of the frequencies is presented in Fig. 6.

At $P=0$ GPa we observe three Raman lines at 120 cm^{-1}, 327 cm^{-1}, and 568 cm^{-1}, respectively. The latter two modes were earlier reported to have frequencies of 331 cm^{-1} and 550 cm^{-1}.[24] The zero-pressure Raman spectrum is dominated by the mode at 327 cm^{-1}. We note that this mode is seen in the Raman spectra of mercury-based high-T_c materials containing HgO as an impurity phase.[25] Increasing the pressure to 0.2 GPa, the 120 cm^{-1} line disappears, and above 0.5 GPa, a Raman line near 167 cm^{-1} becomes clearly resolved.

A somewhat irregular behavior is observed for the two high-frequency modes at very low pressures. The frequency of the 327 cm^{-1} mode increases by about 3 cm^{-1} up to 0.2 GPa and then decreases, while its FWHM first shows a decrease by about 3.5 cm^{-1} up to 0.2 GPa and then increases (see inset to Fig. 6). The 568 cm^{-1} mode shows a similar behavior but less pronounced. The origin of these subtle effects near $P=0$ GPa has not been clarified yet.

Up to 14 GPa, the two high-frequency modes decrease linearly in frequency with increasing pressure. The pressure coefficients are -5.41 cm^{-1}/GPa for the 327 cm^{-1} mode and -2.34 cm^{-1}/GPa for the 568 cm^{-1} mode. The weak frequency increase of the 167 cm^{-1} mode is slightly sublinear with pressure. When the pressure reaches about 14 GPa, the highest-energy mode disappears, a new mode appears near 400 cm^{-1} (pointed out by the arrow in Fig. 5), and the medium-energy Raman line shows a change in pressure coefficient. These discontinuities are consistent with the occurrence of a structural phase transition near 14 GPa. Above 14 GPa, in the high-pressure phase, the two highest-energy modes continue to soften, at rates of -0.77 cm^{-1}/GPa and -2.1 cm^{-1}/GPa, respectively. There are two low-energy Raman lines resolved below 200 cm^{-1} which harden with increasing pressure. Above 28 GPa, the modes between 140 cm^{-1} and 240 cm^{-1} overlap, and their exact frequencies cannot be determined reliably.

A factor group analysis of a *single chain* of orthorhombic HgO has been reported earlier.[24] From such an analysis of the whole unit cell, which contains two chains, we find that there are 12 Raman-active modes ($4A_g$, $2B_{1g}$, $4B_{2g}$, and $2B_{3g}$) and 12 infrared-active modes. Out of the Raman-active modes three are oxygen intrachain modes with A_g, B_{2g}, and B_{3g} symmetry, respectively. We note that the chain mode assigned as B_{1g} in Ref. 24 has B_{2g} symmetry in space group $Pnma$.

In Bi-based superconductors, the frequency of the Bi mode is at about 122 cm^{-1}. Hg has an atomic mass very similar to that of Bi, and the bond length of Hg-O is also very similar to that of Bi-O in Bi-based superconductors; therefore the 120 cm^{-1} mode observed at ambient pressure (see 0 GPa curve in Fig. 5) is assigned as the intrachain mercury mode. The energies of the interchain modes of the low-pressure phase probably are too low in frequency to be observed above our low-frequency limit of 100 cm^{-1}.

We assign the mode at 167 cm^{-1} as the oxygen rotation mode of B_{3g} symmetry, as illustrated in the left bottom corner of Fig. 6. The reasons are that (1) the mercury atom is too heavy to vibrate at such a high frequency and (2) since the chains are relatively isolated from each other at ambient pressure, it is much easier for the oxygen atoms to rotate around the chain than to stretch along the a or c axis. Thus, the energy of the chain rotation mode must be much lower than those of the stretching modes.

The vibrations of the A_g and B_{2g} modes correspond to oxygen displacements along the c_0 and a_0 axes, respectively, as illustrated in Fig. 6. At ambient pressure the Hg-O-Hg bonding angle θ is 109°, and thus the B_{2g} mode shares a larger Hg-O bonding component than the A_g mode. It is mainly this reason that led us to assign a B_{2g} symmetry to the 568 cm^{-1} mode and A_g symmetry to the 327 cm^{-1} mode.

The pressure-induced softening of both the A_g and B_{2g} oxygen intrachain modes is attributed to an increase of the interchain interaction. In particular, the decrease of the interchain distance in the ac plane results in a more pronounced effect of mercury atom potentials in neighboring chains on the vibrational frequencies of the oxygen atoms. Thus, the softening is found to be larger for the mode with the oxygen atoms vibrating along the c axis. The chain structure of orthorhombic HgO reminds us of HgS (cinnabar phase), Se, or Te which have spiral chain structures and show similar phonon softening behavior under pressure.[26–31] Also in these compounds the phonon softening is explained qualitatively by the increasing interchain interactions under pressure as well as a decrease of bond strengths within the chains.

The abrupt drop in frequency for the highest-energy mode at the phase transition is attributed to the loss of the strong covalent Hg-O bond. Since the structure of the high-pressure phase is a distorted variant of the NaCl-type structure, we tentatively associate the two observed oxygen-related modes with LO and TO modes (Raman forbidden in a crystal with center of inversion), which become Raman allowed due to a structural distortion being present in addition to the tetragonal component. The ongoing softening of these modes with increasing pressure may indicate the further approach towards a higher-symmetry structure.

V. EXCITED ELECTRONIC STATES

Figure 7 shows photoluminescence spectra of HgO measured with a Ge detector at different pressures up to 5.5 GPa. At ambient pressure, there are three PL peaks (labeled b, c, and d) in the energy range between 0.5 and 2.0 eV. All three features are attributed to impurity-related near-band-edge states. With increasing pressure, they continuously shift towards lower energy, indicating a decrease of the band gap. We have measured the high-energy edge of the PL emission using a more sensitive photomultiplier detector. The corresponding data (labeled a) are also shown in Fig. 7. The extrapolated zero-pressure energy at 10 K is 2.13 eV, and the pressure coefficient is -0.07 eV/GPa. These results are considered to determine the lower limit for the band gap energy. We note that the sign of this pressure coefficient is opposite to that found for the lowest direct gap in Ge and most zinc-blende-type semiconductors, and the redshift is a factor of 4 larger than that of indirect (Γ-X gap) semiconductors.

We have calculated the electronic energy band structure of HgO using a scalar relativistic tight-binding linear muffin-tin orbital (LMTO) atomic sphere approximation (ASA)

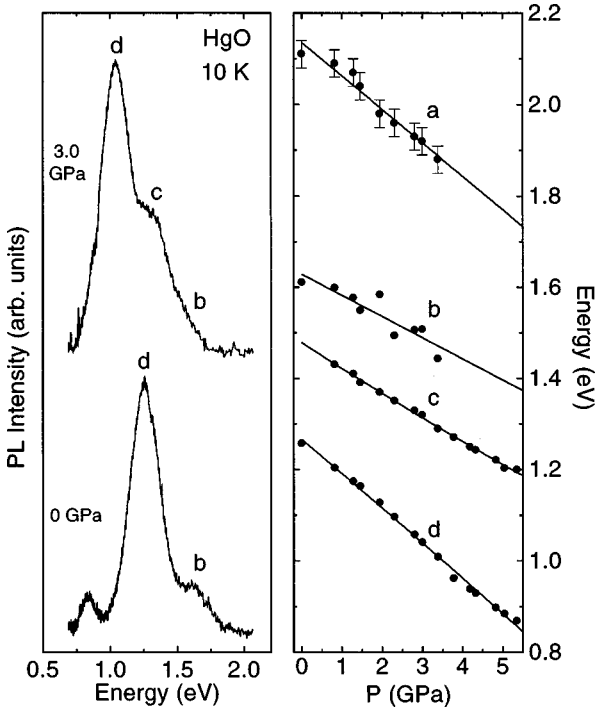

FIG. 7. Left: photoluminescence spectra of HgO at two different pressures ($T=10$ K). Right: PL onset energy (a) and PL peak energies (b–d) as a function of pressure.

scheme.[32] The energy bands corresponding to the ambient pressure structural properties are shown in Fig. 8. The calculated gap energy is 1.33 eV. This value is lower than the experimental lower limit. This is expected to be due to the so-called gap problem inherent to the local-density approximation (LDA) method.[33] The relativistic effects may also contribute to the error. The ordering of bands should not be affected by this error, which implies that HgO is an indirect gap semiconductor at ambient conditions with direct optical transitions being possible at energies slightly higher than the fundamental gap.

Room temperature optical reflectivity (reflectance) spectra at different pressures up to 28 GPa are shown in Fig. 9. At low pressure, the reflectivity spectra show a weak shoulder between 2 and 3 eV. This shoulder is attributed to a sizable oscillator strength just above the band gap due to direct interband transitions. With increasing pressure up to 14 GPa,

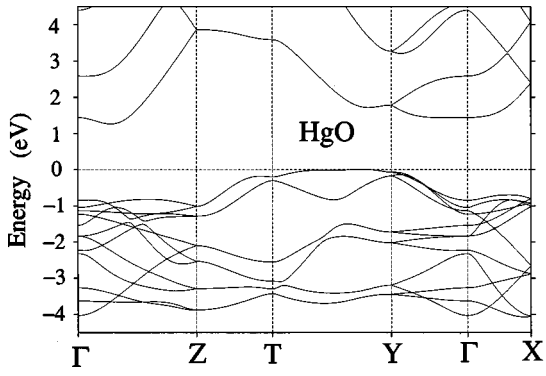

FIG. 8. Scalar relativistic tight-binding LMTO-ASA energy band structure calculated for orthorhombic HgO using the ambient pressure structural parameters.

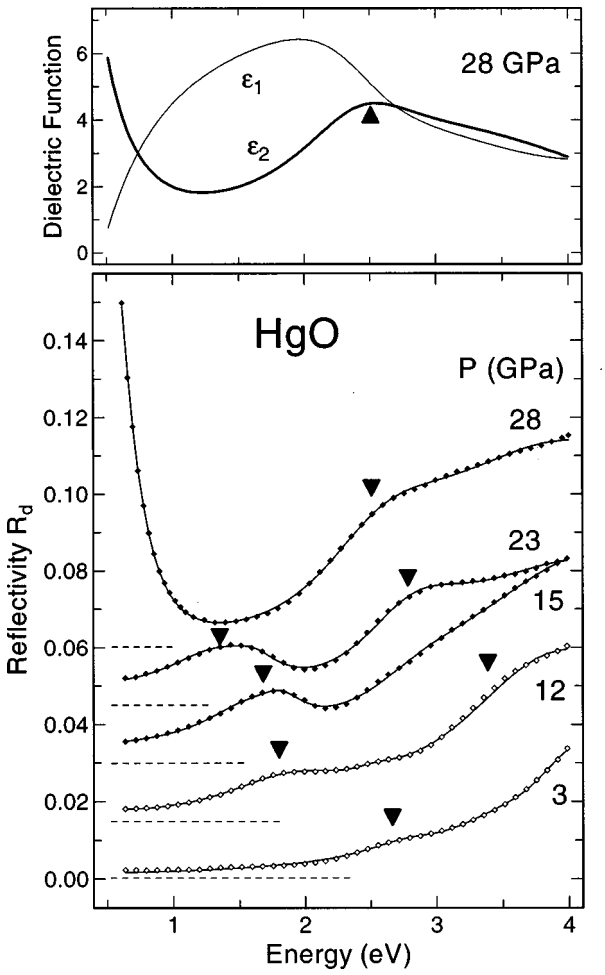

FIG. 9. Optical reflectivity spectra of polycrystalline HgO at different pressures ($T=300$ K). The reflectivity R_d is measured at the interface between diamond window and sample. For clarity, spectra are displaced vertically as indicated by the dashed lines. Solid and open symbols represent a subset of the experimental data points. The solid lines represent results of least squares fits of Drude-Lorentz-type oscillator expressions to the reflectivity spectra (see text). The upper frame shows the real and imaginary parts of the dielectric function obtained from such a fit for the spectrum at 28 GPa. Triangles point to the energies where the imaginary part of the dielectric function exhibits a maximum or edgelike feature.

the reflectivity shoulder shifts down in energy, indicating a reduction of the band gap energy in accordance with the PL results. Near 14 GPa, the outline of the reflectivity spectrum is changed; this is consistent with the structural transition near this pressure value. Upon further compression, the near-infrared reflectivity edge continues to shift down in energy. Near 28 GPa, the optical reflectivity in the infrared regime starts to increase. This signals a significant increase in oscillator strength at low energies. It is attributed to the appearance of free carriers, evidencing a transition to a metallic state.

The real and imaginary parts of the dielectric function $\epsilon(\omega)=\epsilon_1(\omega)+i\epsilon_2(\omega)$ shown in the upper frame of Fig. 9 are obtained from a least squares fit to the reflectivity spectrum at 28 GPa. For this purpose we use the Fresnel relation[34] for the reflectivity R_d at the diamond-sample interface,

$$R_d(\omega)=\left|\frac{n_d(\omega)-\sqrt{\epsilon(\omega)}}{n_d(\omega)+\sqrt{\epsilon(\omega)}}\right|^2, \quad (1)$$

and represent $\epsilon(\omega)$ by a superposition of Drude-Lorentz oscillator expressions,

$$\epsilon(\omega)=1+\omega_P^2\sum_i \frac{f_i}{\omega_i^2-\omega^2-i\Gamma_i\omega}. \quad (2)$$

Here $n_d(\omega)$ is the refractive index of diamond (assumed to be independent of pressure), and f_i, ω_i, and Γ_i are the relative strength ($\Sigma_i f_i=1$), frequency, and damping constant, respectively, of the oscillator with index i. The frequencies ω_i are distributed over the spectral range up to 8 eV. The total oscillator strength is limited by assuming a reasonable unscreened valence electron plasma frequency of $\omega_P=15$ eV. We observe that ϵ_1 tends to cross the zero line at an energy just below 0.5 eV. This low value of the screened plasma frequency indicates a rather low carrier density in the metallic phase, comparable to that in highly doped conventional semiconductors.

The Raman spectra do not show any discontinuous change near 28 GPa both in the outline of the spectra and the Raman line frequencies. Therefore we argue that the transition to the metallic state is continuous. Contrary to the case of the mercury chalcogenides, the semiconductor-to-metal transition in HgO does not seem to result from any major structural change. Since Raman-active modes are still observed at pressure above 28 GPa, the starting structure of metallic HgO is unlikely to be of the NaCl type. The transition to the metallic state is reversible.

VI. CONCLUSIONS

In conclusion, we have investigated the high-pressure behavior of HgO by x-ray powder diffraction, Raman scattering, and electronic state spectroscopies. HgO is found to undergo a phase transition from an orthorhombic to a tetragonal crystal structure at a pressure of 14(1) GPa. The structure of the high-pressure phase is a tetragonally distorted variant of the NaCl-type structure. The x-ray-diffraction results are consistent with an *average* structure of space group $I4/mmm$. However, a disordered or lower-symmetry structure due to displacements of the oxygen atoms from the body-centered positions cannot be ruled out. In the pressure regime below 14 GPa, we observe four Raman-active modes, which are assigned to the irreducible representations of the point group based on a factor group analysis. The two high-frequency oxygen-related modes have negative pressure coefficients. This is attributed to an enhancement of the interchain interaction under pressure going along with a weakening of the Hg-O intrachain bonds. Oxygen modes of the high-pressure phase also soften with increasing pressure, indicating the possibility of another structural phase transition at pressures above 34 GPa, which is the upper pressure limit of the present investigation. Photoluminescence spectra show that the band gap of HgO in the orthorhombic phase decreases with increasing pressure. Optical reflectivity measurements indicate a transition to a metallic state near 28 GPa. We argue that this transition is due to an electron energy band overlap not involving any significant structural change.

ACKNOWLEDGMENTS

We thank U. Oelke, W. Dieterich, and U. Engelhardt for technical assistance. We also thank E. Lacher and E. Schönherr for the growth of single crystals of HgO. One of the authors (T.Z.) acknowledges financial support by the Stiftung Volkswagenwerk.

[1] M. I. McMahon and R. J. Nelmes, Phys. Status Solidi B **198**, 389 (1996), and references therein.

[2] See, e.g., X. Chen, X. Hua, J. Hu, J. M. Langlois, and W. A. Goddard III, Phys. Rev. B **53**, 1377 (1996); A. Mujica, R. J. Needs, and A. Muñoz, Phys. Status Solidi B **198**, 461 (1996); R. Ahuja, P. James, O. Eriksson, J. M. Wills, and B. Johansson, *ibid.* **199**, 75 (1997).

[3] T. Huang and A. L. Ruoff, Phys. Status Solidi A **77**, K193 (1983); Phys. Rev. B **27**, 7811 (1983); J. Appl. Phys. **54**, 5459 (1983).

[4] T. Huang and A. L. Ruoff, Phys. Rev. B **31**, 5976 (1985).

[5] M. I. McMahon, R. J. Nelmes, H. Liu, and S. A. Belmonte, Phys. Rev. Lett. **77**, 1781 (1996).

[6] K. Aurivillius, Acta Chem. Scand. **10**, 852 (1956).

[7] E. A. Decamps, M. Durand, and Y. Marqueton, Opt. Commun. **4**, 358 (1972).

[8] We note that also a yellow form of polycrystalline orthorhombic HgO has been reported. The difference in colors is commonly related to defects or to grain size effects (see Refs. 7 and 9).

[9] M. S. Farag, Z. M. Hanafi, and F. M. Ismail, Z. Phys. Chem. Neue Folge **86**, 1 (1973).

[10] V. B. Singh, Indian J. Pure Appl. Phys. **9**, 367 (1971).

[11] V. V. Shchennikov, Phys. Solid State **35**, 401 (1993).

[12] I. M. Tsidil'kowski, V. V. Shchennikov, and N. G. Gluzman, Sov. Phys. Semicond. **19**, 901 (1985).

[13] V. I. Voronin and V. V. Shchennikov, Sov. Phys. Crystallogr. **34**, 293 (1989).

[14] A. San Miguel, A. Gonzalez Penedo, J. P. Itie, A. Polian, and P. Bordet, in *High Pressure Science and Technology*, edited by W. A. Trzeciakowski (World Scientific, Singapore, 1996), p. 438.

[15] T. Zhou, U. Schwarz, M. Hanfland, Z. Liu, K. Syassen, and M. Cardona, *Proceedings of the 7th International Conference on High Pressure Semiconductor Physics*, Schwäbisch-Gmünd, 1996 [Phys. Status Solidi B **198**, 411 (1996)].

[16] H. K. Mao, J. Xu, and P. M. Bell, J. Geophys. Res. **91**, 4673 (1986).

[17] R. J. Nelmes, P. D. Hatton, M. I. McMahon, R. O. Piltz, J. Crain, R. J. Cernik, and G. Bushnell-Wye, Rev. Sci. Instrum. **63**, 1039 (1992); R. O. Piltz, M. I. McMahon, J. Crain, P. D. Hatton, R. J. Nelmes, R. J. Cernik, and G. Bushnell-Wye, *ibid.* **63**, 700 (1992).

[18] A. Hammersley, computer program Fit2D, ESRF, Grenoble, 1997.

[19] L. G. Akselrud, Yu. Grin, V. K. Pecharsky, P. Y. Pecharsky, and V. S. Fundamenskiy, computer code CSD 4.10, STOE & Cie, Darmstadt, 1992.

[20] K. Syassen and R. Sonnenschein, Rev. Sci. Instrum. **53**, 644 (1982).

[21] M. McMahon (private communication).

[22] W. Klement, A. Jayaraman, and G. C. Kennedy, Phys. Rev. **131**, 1 (1963).

[23] For pure mercury a crystallization pressure of 2 GPa corresponds to a melting temperature of about 60°C [see W. Klement, Jr., A. Jayaraman, and G. C. Kennedy, Phys. Rev. **131**, 1B (1963)]. In the present experiment the melting line of Hg may be affected by impurities, such that the crystallization pressure does not necessarily provide an estimate of the local temperature.

[24] R. P. J. Cooney and J. R. Hall, Aust. J. Chem. **22**, 331 (1969).

[25] M. C. Krantz, C. Thomsen, Hj. Mattausch, and M. Cardona, Phys. Rev. B **50**, 1165 (1994).

[26] A. Werner, H. D. Hochheimer, K. Strössner, and A. Jayaraman, Phys. Rev. B **28**, 3330 (1983).

[27] B. A. Weinstein and R. Zallen, in *Light Scattering in Solids IV*, edited by M. Cardona and G. Güntherodt, Topics in Applied Physics Vol. 54 (Springer, Heidelberg, 1984).

[28] W. Richter, J. B. Renucci, and M. Cardona, Phys. Status Solidi B **56**, 223 (1973).

[29] K. Aoki, O. Shimomura, S. Minomura, N. Koshizuka, and T. Tsushima, J. Phys. Soc. Jpn. **48**, 906 (1980).

[30] R. M. Martin, T. A. Fjeldly, and W. Richter, Solid State Commun. **18**, 865 (1976).

[31] R. M. Martin and G. Lucovsky, Phys. Rev. B **13**, 1383 (1976).

[32] G. Krier, M. van Schilfgaarde, T. A. Paxton, O. Jepson, A. Burkhardt, and O. K. Andersen, computer code TB-LMTO; O. K. Andersen, Z. Pawlowska, and O. Jepsen, Phys. Rev. B **34**, 5253 (1986).

[33] L. J. Sham and M. Schlüter, Phys. Rev. Lett. **51**, 1888 (1983); G. A. Baraff and M. Schlüter, Phys. Rev. B **30**, 3460 (1984).

[34] See, e.g., F. Wooten, *Optical Properties of Solids* (Academic, New York, 1972)